Journal of
Instrumentation

PAPER • **OPEN ACCESS**

Momentum scale calibration of the LHCb spectrometer

To cite this article: R. Aaij *et al* 2024 *JINST* **19** P02008

Published by IOP Publishing for Sissa Medialab

Received: *December 5, 2023*
Accepted: *December 30, 2023*
Published: *February 5, 2024*

Momentum scale calibration of the LHCb spectrometer

The LHCb collaboration

E-mail: mneedham@staffmail.ed.ac.uk

Abstract: For accurate determination of particle masses accurate knowledge of the momentum scale of the detectors is crucial. The procedure used to calibrate the momentum scale of the LHCb spectrometer is described and illustrated using the performance obtained with an integrated luminosity of 1.6 fb^{-1} collected during 2016 in pp running. The procedure uses large samples of $J/\psi \to \mu^+\mu^-$ and $B^+ \to J/\psi K^+$ decays and leads to a relative accuracy of 3×10^{-4} on the momentum scale.

Keywords: Particle tracking detectors; Analysis and statistical methods

ArXiv ePrint: 2312.01772

https://doi.org/10.1088/1748-0221/19/02/P02008

2024 JINST 19 P02008

Contents

1 Introduction

An accurate estimate of the charged-particle momentum scale is a critical ingredient to achieve optimal performance in spectrometers such as the LHCb detector [1]. If the momentum scale is not well calibrated, the measured four-vectors of charged particles will be biased and the measured masses of resonances and other quantities such as decay-time will be shifted from their true values. If the bias is large and depends on the particle kinematics the mass resolution is also degraded, particularly for high mass resonances such as the $\Upsilon(nS)$.

In this paper the procedure used to calibrate the measurement of the charged-particle momentum scale of the LHCb spectrometer from 2011 to 2018 is described and results are presented using data collected during 2016 as an example. Similar results are obtained for other running periods. The paper is arranged as follows. First, the LHCb spectrometer and the formalism used are described. The procedure is then illustrated using a data sample corresponding to an integrated luminosity of $1.6\,\text{fb}^{-1}$, collected in proton-proton (pp) collisions at a centre-of-mass energy of 13 TeV during 2016 data taking. Finally, comparison is drawn with data collected by LHCb during 2012 running and comments are made on addressing biases related to the correlation between the mass and decay time.

2 Detector

The LHCb detector [1, 2] is a single-arm forward spectrometer covering the pseudorapidity range $2 < \eta < 5$, designed for the study of particles containing b or c quarks. The detector includes a high-precision tracking system consisting of a silicon-strip vertex detector (VELO) surrounding

2024 JINST 19 P02008

the pp interaction region [3], a large-area silicon-strip detector (TT) located upstream of a dipole magnet with a bending power of about 4 Tm, and three stations of silicon-strip detectors and straw drift tubes [4] placed downstream of the magnet (T-stations). The length scale of the VELO along the beam axis (the z-direction) is known to a relative precision of 2×10^{-4}. The polarity of the dipole magnet is reversed periodically throughout data-taking. The configuration with the magnetic field vertically upwards, *MagUp* (downwards, *MagDown*), deflects positively (negatively) charged particles in the horizontal plane towards the centre of the LHC. The tracking system provides a measurement of the momentum, p, of charged particles with a relative uncertainty that varies from 0.5% at low momentum to 1.0% at 200 GeV/c.

Different types of charged hadrons are distinguished using information from two ring-imaging Cherenkov detectors [5]. Photons, electrons, and hadrons are identified by a calorimeter system consisting of scintillating-pad and preshower detectors, an electromagnetic calorimeter and a hadronic calorimeter. Muons are identified by a system composed of alternating layers of iron and multiwire proportional chambers [6]. The online event selection is performed by a trigger [7], which consists of a hardware stage, based on information from the calorimeter and muon systems, followed by a software stage, which applies a full event reconstruction including a track fit based on a Kalman filter [8, 9].

In the simulation, pp collisions are generated using Pythia 6.4 [10] with a specific LHCb configuration [11]. Decays of hadronic particles are described by EvtGen [12] in which final state radiation is generated using Photos [13]. The interaction of generated particles with the detector and its response are implemented using the Geant4 toolkit [14] as described in ref. [15].

The accuracy of the momentum scale prior to the procedure described here is determined by the knowledge of the magnetic field map, the alignment, and the detector material. The field of the dipole magnet was mapped to a relative accuracy of 4×10^{-4} with Hall probes prior to first data taking in 2009 [1]. Further measurements were taken during LHC shutdown periods. These measurements were combined with the results of a TOSCA finite-element simulation to provide the field map used in the reconstruction.

The geometry of the LHCb tracking system is relatively complicated and care is needed to achieve the optimal alignment. Detailed metrology and optical surveys were made for all detector components prior to installation. The stability of the C-frames on which the T-stations are mounted are monitored using a CCD-based Rasnik system [4]. During 2014 an additional optical monitoring system (‘BCAM’) was installed to monitor the position of the inner part of this detector [16]. From the information provided by the hardware system and software alignment studies it is known that the position of most detector elements is stable during data taking. An exception is the silicon-strip detector located in the inner part of the first T-station. A shift of ~ 1 cm in the position of this detector along the beam line is seen when the magnet is powered on.

The framework to determine the global alignment of the tracking system is discussed in refs. [17, 18]. It is based on the closed form Kalman filter-based method described in ref. [19]. An important aspect of the software alignment procedure is that it utilizes mass constraints provided by selected $D^0 \to K^+\pi^-$ and $J/\psi \to \mu^+\mu^-$ candidates to reduce weak modes such as the curvature bias described in section 3 and ref. [20]. During Run 1 (2010–2012) updates to the alignment constants were made offline when significant changes to the running conditions occurred (e.g. changes in magnet polarity). From 2015 onwards (Run 2) the alignment runs in real-time each fill at the software trigger stage, using the D^0 mass constraint, and the constants are automatically updated if significant changes are detected [21]. Midway through the 2018 run period a high-granularity alignment of the spectrometer was made using a sample of high-momentum muons produced in $Z^0 \to \mu^+\mu^-$ decays. The resulting alignment was then used as an input to the online procedure.

A correction for energy loss in the detector material is applied during the Kalman filter step. This correction uses the Bethe formula including the density correction [22]. As particle identification information is not available when the track fit is performed, all particles are considered to be pions. This is a valid assumption as particles that traverse the full spectrometer are highly relativistic ($p > 3\,\text{GeV}/c$) such that the energy loss correction is independent of the particle type. The size of the applied correction is momentum dependent and comparable to the intrinsic momentum resolution of the detector. The amount of material in the detector is known from surveys and assays during installation to a precision of $5 - 10\,\%$ [2]. In detailed studies of particles' masses, an additional uncertainty to the momentum scale determination that accounts for the material knowledge is assigned [23].

From the above discussion it is clear that to achieve an accurate calibration of the momentum scale using the decays of precisely measured resonances are needed. The methodology for this will be detailed in the next section.

3 Formalism

Consider a two-body decay $P \to d_1 d_2$. The invariant mass of the system, in natural units, is

$$m_{12} = \sqrt{m_1^2 + m_2^2 + 2(E_1 E_2 - \vec{p}_1 \cdot \vec{p}_2)}, \tag{3.1}$$

where $m_{1,2}$, $\vec{p}_{1,2}$, $E_{1,2}$ are respectively the mass, momentum vector and energy of the decay products. The derivative of this expression with respect to the magnitude of the momentum vector $p_1 = |\vec{p}_1|$ can be written as

$$\frac{\mathrm{d}m_{12}}{\mathrm{d}p_1} = \frac{m_{12}^2 - m_1^2 - m_2^2 - 2m_1^2 E_2/E_1}{2\,m_{12}\,p_1}. \tag{3.2}$$

Consequently, if the momentum scale of child d_1 is biased by a scale factor

$$p_1 \to (1 + \alpha_1)\,p_1. \tag{3.3}$$

The observed change in the two-body invariant mass, to first order in α_1, is given by

$$m_{12} \to m_{12} + \alpha_1 \frac{m_{12}^2 - m_1^2 - m_2^2 - 2m_1^2 E_2/E_1}{2m_{12}}. \tag{3.4}$$

Therefore, the value of α_1 can be obtained from the difference δm between the observed average invariant mass m_{12} and the known mass of the parent particle m_P.

In general a momentum-scale bias will affect both child particles. To first order in the momentum-scale bias the total mass bias can be obtained by summing the two contributions. Assuming the momentum-scale bias is the same for both children (that is $\alpha_1 = \alpha_2$), the observed bias in the mass is given by

$$\delta m = \alpha\,\frac{m_P^2 - m_1^2 - m_2^2 - m_1^2 E_2/E_1 - m_2^2 E_1/E_2}{m_P}. \tag{3.5}$$

In the case of two identical child particles with mass m, the average bias is

$$\delta m = \alpha \, \frac{m_P^2 - m^2 R}{m_P}, \tag{3.6}$$

with

$$R = 2 + \frac{E_1}{E_2} + \frac{E_2}{E_1}. \tag{3.7}$$

Equation 3.6 is appropriate for decays such as $K^0_S \to \pi^+\pi^-$ where the mass of the child particles is comparable to the mass of the parent. For the decays $J/\psi \to \mu^+\mu^-$ and $\Upsilon(nS) \to \mu^+\mu^-$, measured in the LHCb detector, $m^2 R \ll m_P^2$ and hence

$$\Delta m \approx \alpha \cdot m_P. \tag{3.8}$$

The $B^+ \to J/\psi K^+$ decay mode,[1] with the subsequent $J/\psi \to \mu^+\mu^-$ decay, is crucial for the calibration of the LHCb spectrometer. For this decay, after applying a kinematic fit [24] that constrains the measured dimuon mass to the known J/ψ mass, the mass resolution is dominated by the knowledge of the momentum of the kaon. Consequently, it is reasonable to assume that the reconstructed B^+ mass is directly related to the momentum scale of the charged kaon. Labelling the kaon momentum by p_1 the momentum-scale bias is obtained using the average value of the mass bias corrected by the kinematic factor in eq. 3.4,

$$\alpha \;=\; (m_{12} - m_P)\, \frac{2m_{12}}{m_{12}^2 - m_1^2 - m_2^2 - 2m_1^2 E_2/E_1}. \tag{3.9}$$

This method gives the momentum-scale in bins of the kaon kinematics. The momentum p_2 of the mass-constrained J/ψ is considered to be unaffected by the momentum-scale bias. Studies with the $B^+ \to J/\psi K^+$ simulation indicate that this assumption is valid to a precision of 10^{-4} in the parameter α.

A momentum-scale bias as discussed above is generated by a wrong estimation of the magnetic field integral or a poor tuning of the energy loss correction in the detector. Another possible effect is the curvature bias due to detector misalignment discussed in ref. [20]. For the LHCb geometry, a typical misalignment that leads to a curvature bias is a small displacement, in the bending plane, of the T-stations relative to the VELO. Defining the curvature of particle i as $\omega_i = q_i/p_i$, where q_i is the particle charge, the effect of a curvature bias $\omega_1 \to \omega_1 + \delta\omega$ on the two-body invariant mass follows from eq. 3.4 as

$$\delta m_{12} = -\delta\omega \, \frac{p_1}{q_1} \, \frac{m_{12}^2 - m_1^2 - m_2^2 - 2m_1^2 E_2/E_1}{2m_{12}}. \tag{3.10}$$

Contrary to a global momentum-scale bias, the mass bias due to a curvature bias has opposite sign for the particles in a two-body decay. If the two particles have equal momentum, the two contributions exactly cancel. Labelling the momentum of the negatively charged child as p_1, in the limit of massless children eq. 3.10 becomes

$$\delta m_{12} = \frac{1}{2}\delta\omega \, m_{12}\, (p_1 - p_2). \tag{3.11}$$

[1]Charge conjugation is implied throughout.

2024 JINST 19 P02008

Hence, a curvature bias can be identified by considering the average invariant mass as a function of the momentum difference between the children.

A curvature bias leads to a relative momentum bias that is quadratic in the momentum. As a result momentum-scale bias effects typically dominate at small momenta, while curvature bias effects dominate at large momenta. For the LHCb detector, the curvature bias from residual misalignment needs to be accounted for in electroweak physics measurements, such as the W-boson mass measurement detailed in ref. [25, 26]. Applying an additional correction for curvature bias effects has little impact on the results presented here.

4 Radiative corrections and momentum scale calibration

A complication that arises in the extraction of the momentum scale from resonance decays is due to QED final state radiation. This has two effects. First, it introduces a long radiative tail that must be accounted for to obtain a good quality fit. A common approach is to fit a Crystal Ball function [27] which has a Gaussian core and a power-law tail. The Crystal Ball function has four parameters: mean (μ), resolution (σ), transition point for the radiative tail (a) and the exponent of the power law (n). The latter three parameters are highly correlated and care is needed to obtain a reliable fit. The procedure adopted is to fix n to one and parameterize a from fits to the shape obtained from the generator-level simulation convolved with a Gaussian resolution function with known σ. As an example, the resulting quadratic function for the $J/\psi \to \mu^+\mu^-$ decay mode is shown in figure 1(left).

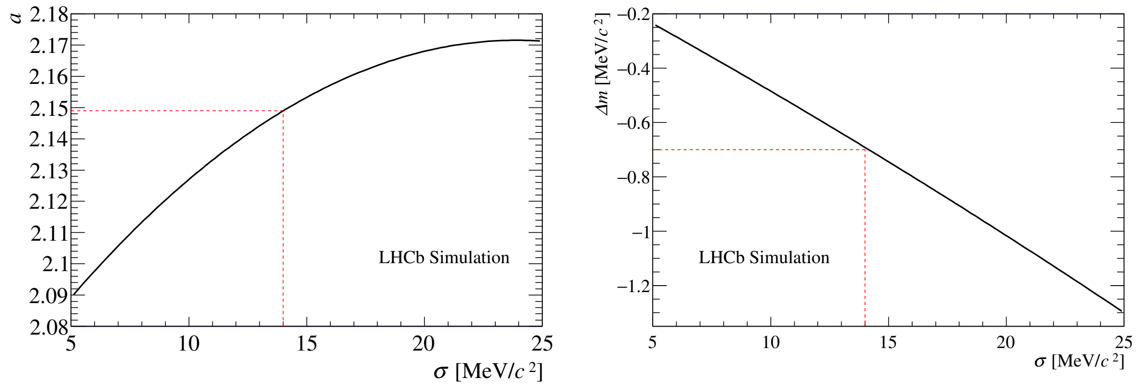

Figure 1. (left) Parameterization of a and (right) bias on the measured mass versus σ for the $J/\psi \to \mu^+\mu^-$ decay mode. The (red) dashed lines highlight the values for the typical J/ψ mass resolution of 14 MeV/c^2.

The second effect of final state radiation is to shift the position of the mass peak to lower values. This bias remains even if a fit to a Crystal Ball function is made since it has a symmetric Gaussian core. It is corrected for by parameterizing the observed bias in the simulation as a function of the resolution. Figure 1(right) shows the resulting correction for the $J/\psi \to \mu^+\mu^-$ decay mode. The typical correction size is 0.7 MeV/c^2, which corresponds to $\alpha \sim 2 \times 10^{-4}$. The reliability of the Photos simulation is probed by varying its settings leading to a relative uncertainty of 5×10^{-5} on the momentum scale determination.

2024 JINST 19 P02008

5 Method

The procedure used to correct the momentum scale exploits the large samples of detached $J/\psi \rightarrow \mu^+\mu^-$ and $B^+ \rightarrow J/\psi K^+$ decays collected by LHCb. The calibration is performed separately for each year of data taking and is illustrated here using data collected during 2016. Corrections are performed that account for the variation of the momentum scale with time, Δ_r, particle kinematics, Δ_k, and to fix the global momentum scale, Δ_g. In the first step the data sample is divided into run periods chosen according to known changes in conditions (e.g. reversals of the magnet polarity) or known drifts in the measured J/ψ mass. For each run period a fit is made to the dimuon invariant mass distribution of selected J/ψ candidates. In this fit the signal is modelled by a Crystal Ball function with the tail parameterisation described in section 4 and the background by an exponential function. The fitted mean mass value is corrected for the effect of radiative corrections and converted into Δ_r using eq. 3.8. In figure 2 (left) it can be seen that the size of Δ_r varies from $1 - 4 \times 10^{-4}$ over the 2016 running period. Two trends are visible. At the start of the 2016 run period a global upwards drift of Δ_r is observed. This is correlated with movements of the hardware monitoring systems of the downstream tracking stations over time [4]. In addition, Δ_r for data taken with *MagUp* is generally larger than *MagDown* by $\sim 10^{-4}$. A similar effect is observed in all LHCb running during Run 1 and 2. It may be due to the shifts in the T-station positions when the field is reversed as discussed in section 2 or to movements of the magnet coils.

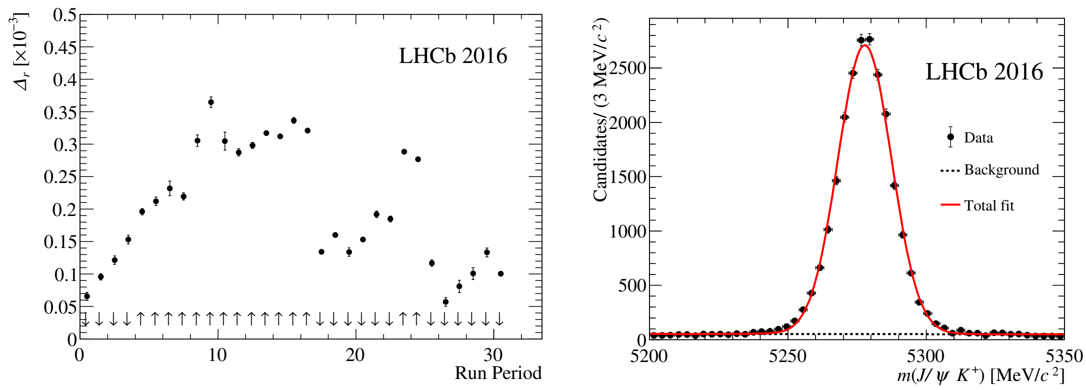

Figure 2. (left) Variation of Δ_r, during the 2016 run period determined using the $J/\psi \rightarrow \mu^+\mu^-$ decay mode. The magnetic field polarity is indicated below the plot with the symbols $\uparrow, \downarrow$ for field up and down respectively. (right) Example fit to the $J/\psi K^+$ invariant mass distribution for candidates with $q \cdot f_p > 0$ and $0.025 < tx < 0.05$ rad and $0 < ty < 0.05$ rad for the 2016 dataset.

The next step is to determine Δ_k. Fits are made to the invariant mass distribution of $B^+ \rightarrow J/\psi K^+$ candidates in bins of the kaon kinematics and the field scale determined by converting the fitted value of the B^+ mass into an estimate of the momentum scale using eq. 3.9. Ideally, the phase space would be binned according to the kaon track slopes ($tx = \tan^{-1}(p_x/p_z)$ and $ty = \tan^{-1}(p_y/p_z)$) and curvature (q/p). With the available dataset size this is not possible. Various binning schemes and reduced sets of variables were explored. The best performance, judged by the improvement in the mass resolution for the $\Upsilon(nS)$ resonances, was obtained by dividing the data according to the sign of

2024 JINST 19 P02008

the product of the track charge and magnetic field polarity,[2] $q \cdot f_p$, and binning according to tx and ty. The binning scheme for each year was adjusted such that statistical uncertainty on each bin was $O(10^{-4})$. An example mass fit to the $B^+ \to J/\psi K^+$ mode is shown in figure 2 (right). The resulting correction maps are shown in figure 3. Particularly at the edge of the detector the values of Δ_k are large ($\Delta_k \sim 10^{-3}$). Local corrections to the momentum scale at the level of 10^{-3} are needed.

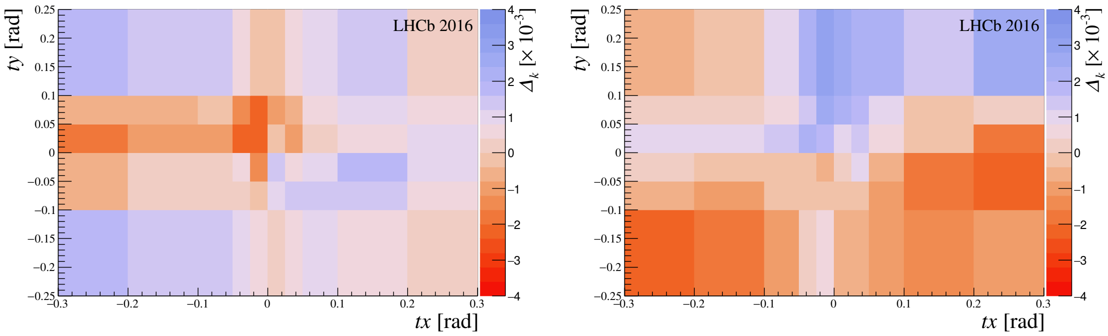

Figure 3. Local momentum scale correction Δ_k as a function of tx and ty for the 2016 dataset (left) $q \cdot f_p > 0$ and (right) $q \cdot f_p < 0$.

The final step is to fix, Δ_g, the global momentum scale. This is done by fitting the $J/\psi \to \mu^+\mu^-$ dataset with a signal described by the sum of two Crystal Ball functions and an exponential background component. The J/ψ mass distribution after this calibration is shown in figure 4.

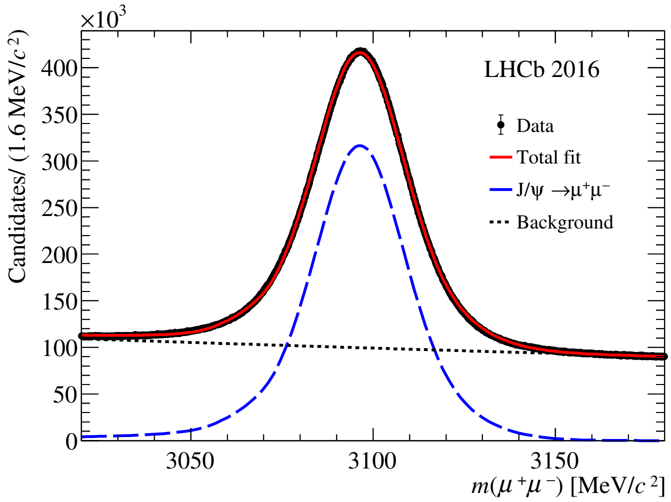

Figure 4. Fit to the dimuon invariant mass distribution for the J/ψ sample after the procedure discussed in the text. The signal (dashed blue line), combinatorial background (dotted black line) and total fit mode (red line) are superimposed.

The total momentum scale correction applied to each particle is thus

$$1 - \alpha = 1 - \Delta_g - \Delta_k - \Delta_r \,.$$

[2] $f_p = -1$ for *MagDown* and 1 for *MagUp*.

2024 JINST 19 P02008

6 Validation

Cross-checks are made of the validity of the calibration procedure using the $J/\psi \to \mu^+\mu^-$ and $B^+ \to J/\psi K^+$ samples together with a sample of $\Upsilon(nS)$ decays shown in figure 5 (left). The large samples available allow the variation of the momentum scale to be studied as a function of kinematic variables such as p, transverse momentum and the orientation of the decay plane with respect to the magnetic field. As an example, figure 5 (right) shows the remaining bias on the momentum scale as a function of p_d which is the momentum of the kaon for the $B^+ \to J/\psi K^+$ sample and half the momentum of the parent in the case of the J/ψ and $\Upsilon(1S)$ resonances. It can be seen that the variation of α as a function of momentum is less than 3×10^{-4}.

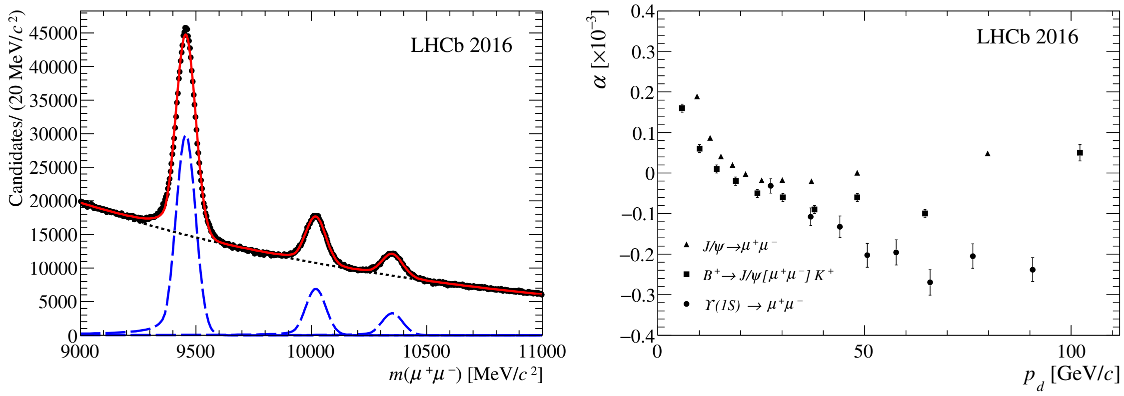

Figure 5. (left) Fit to the sample of selected dimuon candidates in the region of the Υ resonances. Each Υ resonance is described by a Crystal Ball function (blue dashed line) and the combinatorial background by an exponential (black dotted line). The total fit model is also superimposed. (right) Bias on the momentum scale, α versus p_d as defined in the text for the $J/\psi \to \mu^+\mu^-$, $B^+ \to J/\psi K^+$ and the $\Upsilon(1S) \to \mu^+\mu^-$ samples.

The size of Δ_k, is similar in magnitude to the momentum resolution. As can be seen in table 1 applying the calibration improves the relative mass resolution for the $\Upsilon(nS)$ resonances by around 5%.

Table 1. Invariant mass resolution for the Υ resonances before and after the momentum scale calibration.

Resonance	Mass resolution [MeV/c^2]	
	Before	After
$\Upsilon(1S)$	44.4 ± 0.1	42.4 ± 0.1
$\Upsilon(2S)$	45.9 ± 0.3	43.9 ± 0.2
$\Upsilon(3S)$	47.3 ± 0.5	45.2 ± 0.5

Various checks are made using the $B^+ \to J/\psi K^+$ sample. For example, dividing the data according to whether the kaon has hits in the TT detector, whether it traversed the inner or outer parts of the downstream tracker and the location of its first measurements in the vertex detector. In these tests no evidence of a bias significantly larger than the 3×10^{-4} level was found in any kinematic region.

Figure 6 summarizes the residual bias observed for a variety of different decay modes that probe a range of particle kinematics. It can be seen that the variation in α between the different modes again does not exceed 3×10^{-4}.

Based upon the observed variation of α seen for different decay-modes and as function of particle kinematics the uncertainty on α is taken to be 3×10^{-4}. A similar conclusion is drawn by considering the variation in the observed D^0 mass in four-body decay modes [23].

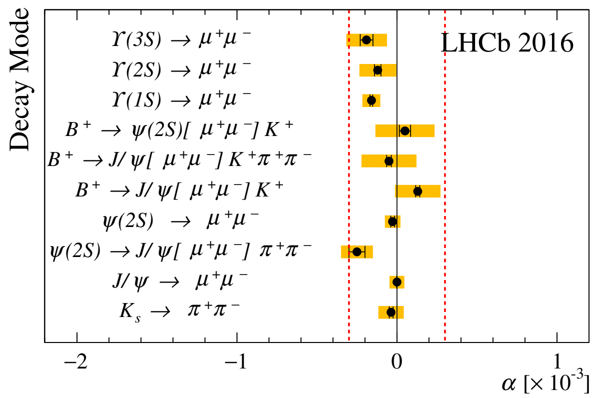

Figure 6. Average momentum-scale bias α determined from the reconstructed mass of various decay modes after the momentum calibration procedure for the 2016 dataset. The K^0_S decays considered are those that occur in the vertex detector and have a flight distance of less than 5 cm. The black error bars represent the statistical uncertainty whilst the (yellow) filled areas also include contributions to the systematic uncertainty from the fitting procedure, the effect of QED radiative corrections, and the uncertainty on the mass of the decaying meson [22]. The (red) dashed lines show the assigned uncertainty of $\pm 3 \times 10^{-3}$ on the momentum scale.

7 Comparison with Run 1

The procedure described here was used to calibrate Run 1 data (see for example ref. [23, 28]). The main difference between the two datasets is the size of the overall correction. For the Run 1 data taking an earlier and less accurate version of the magnetic field map was used. With this field map values of Δ_r around 1×10^{-3} were found. After the momentum scale calibration a similar performance to the 2016 data is achieved. This can be seen in figure 7 where the residual bias for a variety of decay modes is summarized for the study of the 2012 data.

8 Selection biases

An additional invariant mass bias is present for open charm decays selected with cuts on quantities related to the flight distance. This can be seen by considering a two-body decay such as $D^0 \to K^-\pi^+$. If multiple scattering, that occurs within the RF-foil that separates the VELO from the primary LHC vacuum, increases the opening angle between the decay products, both the reconstructed invariant mass and the decay length will be higher than the true value. Thus if cuts are applied on the minimum flight distance candidates with higher values of invariant mass are selected. The size of this bias depends on the selection and the lifetime of the decaying hadron. If no lifetime biasing cuts are applied or the particles are prompt (such as the $\Upsilon(nS)$) or long-lived (like b-hadrons), the size of this effect is negligible. The lifetime of open charm hadrons is such that with typical selections a large bias is seen. With the selection applied in the trigger [21] the size of this bias is estimated

2024 JINST 19 P02008

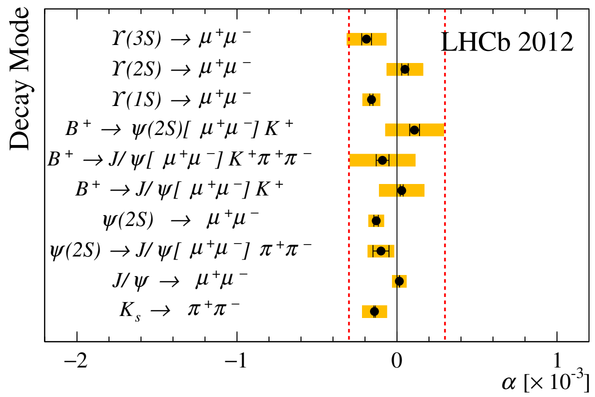

Figure 7. Average momentum-scale bias α determined from the reconstructed mass of various decay modes after the momentum calibration procedure for data collected in 2012. The K^0_S decays considered are those that occur in the vertex detector and have a flight distance of less than 5 cm. The black error bars represent the statistical uncertainty whilst the (yellow) filled areas also include contributions to the systematic uncertainty from the fitting procedure, the effect of QED radiative corrections, and the uncertainty on the mass of the decaying meson. The (red) dashed lines show the assigned uncertainty of $\pm 3 \times 10^{-3}$ on the momentum scale.

using the simulation to be 0.7 MeV/c^2 and 0.2 MeV/c^2 for the D^0 and D^+ mesons respectively. The difference in the size of the bias reflects the difference in the lifetime of the two mesons. Several approaches to correct this are adopted. For the studies of open charm meson masses presented in ref. [23] a lifetime unbiased selection is used. In other analyses, such as the discovery of the Ξ^{++}_{cc} baryon [29], tight requirements on lifetime related variables are needed. In such cases the bias is studied and corrected using the simulation.

9 Summary

In this paper the calibration of the momentum scale of the LHCb detector has been described and illustrated using data collected during 2016. The procedure used is generic and makes use of the large $J/\psi \to \mu^+\mu^-$ and $B^+ \to J/\psi K^+$ samples that have been collected. The uncertainty on the procedure is judged to be 3×10^{-3} by studying the decays of well known resonances. Similar performance is achieved for the other years in Run 2. The method has allowed the LHCb collaboration to make many precise determinations of particle masses and widths over the last decade. Further improvements are possible with a better understanding of the field map and detector material.

Acknowledgments

We express our gratitude to our colleagues in the CERN accelerator departments for the excellent performance of the LHC. We thank the technical and administrative staff at the LHCb institutes. We acknowledge support from CERN and from the national agencies: CAPES, CNPq, FAPERJ and FINEP (Brazil); MOST and NSFC (China); CNRS/IN2P3 (France); BMBF, DFG and MPG (Germany); INFN (Italy); NWO (Netherlands); MNiSW and NCN (Poland); MCID/IFA (Romania); MICINN (Spain); SNSF and SER (Switzerland); NASU (Ukraine); STFC (United Kingdom); DOE NP and NSF (U.S.A.). We acknowledge the computing resources that are provided by CERN, IN2P3 (France), KIT and

DESY (Germany), INFN (Italy), SURF (Netherlands), PIC (Spain), GridPP (United Kingdom), CSCS (Switzerland), IFIN-HH (Romania), CBPF (Brazil), and Polish WLCG (Poland). We are indebted to the communities behind the multiple open-source software packages on which we depend. Individual groups or members have received support from ARC and ARDC (Australia); Key Research Program of Frontier Sciences of CAS, CAS PIFI, CAS CCEPP, Fundamental Research Funds for the Central Universities, and Sci. & Tech. Program of Guangzhou (China); Minciencias (Colombia); EPLANET, Marie Skłodowska-Curie Actions, ERC and NextGenerationEU (European Union); A*MIDEX, ANR, IPhU and Labex P2IO, and Région Auvergne-Rhône-Alpes (France); AvH Foundation (Germany); ICSC (Italy); GVA, XuntaGal, GENCAT, Inditex, InTalent and Prog. Atracción Talento, CM (Spain); SRC (Sweden); the Leverhulme Trust, the Royal Society and UKRI (United Kingdom).

References

[1] LHCb collaboration, *The LHCb Detector at the LHC*, 2008 *JINST* **3** S08005.

[2] LHCb collaboration, *LHCb Detector Performance*, *Int. J. Mod. Phys. A* **30** (2015) 1530022 [arXiv:1412.6352].

[3] R. Aaij et al., *Performance of the LHCb Vertex Locator*, 2014 *JINST* **9** P09007 [arXiv:1405.7808].

[4] LHCb Outer Tracker group, *Performance of the LHCb Outer Tracker*, 2014 *JINST* **9** P01002 [arXiv:1311.3893].

[5] LHCb RICH collaboration, *Performance of the LHCb RICH detector at the LHC*, *Eur. Phys. J. C* **73** (2013) 2431 [arXiv:1211.6759].

[6] A.A. Alves Jr. et al., *Performance of the LHCb muon system*, 2013 *JINST* **8** P02022 [arXiv:1211.1346].

[7] R. Aaij et al., *The LHCb Trigger and its Performance in 2011*, 2013 *JINST* **8** P04022 [arXiv:1211.3055].

[8] R.E. Kalman, *A New Approach to Linear Filtering and Prediction Problems*, *J. Basic Eng.* **82** (1960) 35.

[9] R. Fruhwirth, *Application of Kalman filtering to track and vertex fitting*, *Nucl. Instrum. Meth. A* **262** (1987) 444.

[10] T. Sjostrand, S. Mrenna and P.Z. Skands, *PYTHIA 6.4 Physics and Manual*, *JHEP* **05** (2006) 026 [hep-ph/0603175].

[11] I. Belyaev et al., *Handling of the generation of primary events in Gauss, the LHCb simulation framework*, *J. Phys. Conf. Ser.* **331** (2011) 032047.

[12] D.J. Lange, *The EvtGen particle decay simulation package*, *Nucl. Instrum. Meth. A* **462** (2001) 152.

[13] P. Golonka and Z. Was, *PHOTOS Monte Carlo: A precision tool for QED corrections in Z and W decays*, *Eur. Phys. J. C* **45** (2006) 97 [hep-ph/0506026].

[14] J. Allison et al., *Geant4 developments and applications*, *IEEE Trans. Nucl. Sci.* **53** (2006) 270.

[15] M. Clemencic et al., *The LHCb simulation application, Gauss: Design, evolution and experience*, *J. Phys. Conf. Ser.* **331** (2011) 032023.

[16] J.-C. Gayde et al., *Alignment and Monitoring Systems for Accelerators and Experiments Based on BCAM - First Results and Benefits of Systems Developed for ATLAS, LHCb and HIE-ISOLDE*, in the proceedings of the *9th International Particle Accelerator Conference*, Vancouver, Canada, 29 April–4 May 2018 [DOI:10.18429/JACoW-IPAC2018-WEPAF067].

[17] J. M. Amoraal, *Alignment of the LHCb detector with Kalman filter fitted tracks*, *J. Phys. Conf. Ser.* **219** (2010) 032028.

[18] M. Deissenroth, *Experience with LHCb alignment software on first data*, *J. Phys. Conf. Ser.* **219** (2010) 032035.

[19] W. Hulsbergen, *The global covariance matrix of tracks fitted with a Kalman filter and an application in detector alignment*, *Nucl. Instrum. Meth. A* **600** (2009) 471 [arXiv:0810.2241].

[20] J. Amoraal et al., *Application of vertex and mass constraints in track-based alignment*, *Nucl. Instrum. Meth. A* **712** (2013) 48 [arXiv:1207.4756].

[21] G. Dujany and B. Storaci, *Real-time alignment and calibration of the LHCb Detector in Run II*, *J. Phys. Conf. Ser.* **664** (2015) 082010.

[22] Particle Data group, *Review of Particle Physics*, *Prog. Theor. Exp. Phys.* **2022** (2022) 083C01.

[23] LHCb collaboration, *Precision measurement of D meson mass differences*, *JHEP* **06** (2013) 065 [arXiv:1304.6865].

[24] W.D. Hulsbergen, *Decay chain fitting with a Kalman filter*, *Nucl. Instrum. Meth. A* **552** (2005) 566 [physics/0503191].

[25] LHCb collaboration, *Measurement of the W boson mass*, *JHEP* **01** (2022) 036 [arXiv:2109.01113].

[26] LHCb collaboration, *Charge-dependent curvature-bias corrections using a pseudomass method*, arXiv:2311.04670.

[27] T. Skwarnicki, *A study of the radiative CASCADE transitions between the Upsilon-Prime and Upsilon resonances*, Ph.D. thesis, INP, Cracow, Poland (1986).

[28] LHCb collaboration, *Measurement of the Λ_b^0, Ξ_b^- and Ω_b^- baryon masses*, *Phys. Rev. Lett.* **110** (2013) 182001 [arXiv:1302.1072].

[29] LHCb collaboration, *Observation of the doubly charmed baryon Ξ_{cc}^{++}*, *Phys. Rev. Lett.* **119** (2017) 112001 [arXiv:1707.01621].

The LHCb collaboration

R. Aaij[35], A.S.W. Abdelmotteleb[54], C. Abellan Beteta[48], F. Abudinén[54], T. Ackernley[58], B. Adeva[44], M. Adinolfi[52], P. Adlarson[78], C. Agapopoulou[46], C.A. Aidala[79], Z. Ajaltouni[11], S. Akar[63], K. Akiba[35], P. Albicocco[25], J. Albrecht[17], F. Alessio[46], M. Alexander[57], A. Alfonso Albero[43], Z. Aliouche[60], P. Alvarez Cartelle[53], R. Amalric[15], S. Amato[3], J.L. Amey[52], Y. Amhis[13,46], L. An[6], L. Anderlini[24], M. Andersson[48], A. Andreianov[41], P. Andreola[48], M. Andreotti[23], D. Andreou[66], A. Anelli[28,o], D. Ao[7], F. Archilli[34,u], M. Argenton[23], S. Arguedas Cuendis[9], A. Artamonov[41], M. Artuso[66], E. Aslanides[12], M. Atzeni[62], B. Audurier[14], D. Bacher[61], I. Bachiller Perea[10], S. Bachmann[19], M. Bachmayer[47], J.J. Back[54], P. Baladron Rodriguez[44], V. Balagura[14], W. Baldini[23], J. Baptista de Souza Leite[2], M. Barbetti[24,l], I.R. Barbosa[67], R.J. Barlow[60], S. Barsuk[13], W. Barter[56], M. Bartolini[53], J. Bartz[66], F. Baryshnikov[41], J.M. Basels[16], G. Bassi[32,r], B. Batsukh[5], A. Battig[17], A. Bay[47], A. Beck[54], M. Becker[17], F. Bedeschi[32], I.B. Bediaga[2], A. Beiter[66], S. Belin[44], V. Bellee[48], K. Belous[41], I. Belov[26], I. Belyaev[41], G. Benane[12], G. Bencivenni[25], E. Ben-Haim[15], A. Berezhnoy[41], R. Bernet[48], S. Bernet Andres[42], C. Bertella[60], A. Bertolin[30], C. Betancourt[48], F. Betti[56], J. Bex[53], Ia. Bezshyiko[48], J. Bhom[38], M.S. Bieker[17], N.V. Biesuz[23], P. Billoir[15], A. Biolchini[35], M. Birch[59], F.C.R. Bishop[10], A. Bitadze[60], A. Bizzeti, M.P. Blago[53], T. Blake[54], F. Blanc[47], J.E. Blank[17], S. Blusk[66], D. Bobulska[57], V. Bocharnikov[41], J.A. Boelhauve[17], O. Boente Garcia[14], T. Boettcher[63], A. Bohare[56], A. Boldyrev[41], C.S. Bolognani[76], R. Bolzonella[23,k], N. Bondar[41], F. Borgato[30,46], S. Borghi[60], M. Borsato[28,o], J.T. Borsuk[38], S.A. Bouchiba[47], T.J.V. Bowcock[58], A. Boyer[46], C. Bozzi[23], M.J. Bradley[59], A. Brea Rodriguez[44], N. Breer[17], J. Brodzicka[38], A. Brossa Gonzalo[44], J. Brown[58], D. Brundu[29], A. Buonaura[48], L. Buonincontri[30], A.T. Burke[60], C. Burr[46], A. Bursche[69], A. Butkevich[41], J.S. Butter[53], J. Buytaert[46], W. Byczynski[46], S. Cadeddu[29], H. Cai[71], R. Calabrese[23,k], L. Calefice[17], S. Cali[25], M. Calvi[28,o], M. Calvo Gomez[42], J. Cambon Bouzas[44], P. Campana[25], D.H. Campora Perez[76], A.F. Campoverde Quezada[7], S. Capelli[28,o], L. Capriotti[23], R. Caravaca-Mora[9], A. Carbone[22,i], L. Carcedo Salgado[44], R. Cardinale[26,m], A. Cardini[29], P. Carniti[28,o], L. Carus[19], A. Casais Vidal[62], R. Caspary[19], G. Casse[58], J. Castro Godinez[9], M. Cattaneo[46], G. Cavallero[23], V. Cavallini[23,k], S. Celani[19], J. Cerasoli[12], D. Cervenkov[61], S. Cesare[27,n], A.J. Chadwick[58], I. Chahrour[79], M. Charles[15], Ph. Charpentier[46], C.A. Chavez Barajas[58], M. Chefdeville[10], C. Chen[12], S. Chen[5], Z. Chen[7], A. Chernov[38], S. Chernyshenko[50], V. Chobanova[44,y], S. Cholak[47], M. Chrzaszcz[38], A. Chubykin[41], V. Chulikov[41], P. Ciambrone[25], M.F. Cicala[54], X. Cid Vidal[44], G. Ciezarek[46], P. Cifra[46], P.E.L. Clarke[56], M. Clemencic[46], H.V. Cliff[53], J. Closier[46], J.L. Cobbledick[60], C. Cocha Toapaxi[19], V. Coco[46], J. Cogan[12], E. Cogneras[11], L. Cojocariu[40], P. Collins[46], T. Colombo[46], A. Comerma-Montells[43], L. Congedo[21], A. Contu[29], N. Cooke[57], I. Corredoira [44], A. Correia[15], G. Corti[46], J.J. Cottee Meldrum[52], B. Couturier[46], D.C. Craik[48], M. Cruz Torres[2,g], E. Curras Rivera[47], R. Currie[56], C.L. Da Silva[65], S. Dadabaev[41], L. Dai[68], X. Dai[6], E. Dall'Occo[17], J. Dalseno[44], C. D'Ambrosio[46], J. Daniel[11], A. Danilina[41], P. d'Argent[21], A. Davidson[54], J.E. Davies[60], A. Davis[60], O. De Aguiar Francisco[60], C. De Angelis[29,j], J. de Boer[35], K. De Bruyn[75], S. De Capua[60], M. De Cian[19,46], U. De Freitas Carneiro Da Graca[2,b], E. De Lucia[25], J.M. De Miranda[2], L. De Paula[3], M. De Serio[21,h], D. De Simone[48],

2024 JINST 19 P02008

P. De Simone[25], F. De Vellis[17], J.A. de Vries[76], F. Debernardis[21,h], D. Decamp[10], V. Dedu[12], L. Del Buono[15], B. Delaney[62], H.-P. Dembinski[17], J. Deng[8], V. Denysenko[48], O. Deschamps[11], F. Dettori[29,j], B. Dey[74], P. Di Nezza[25], I. Diachkov[41], S. Didenko[41], S. Ding[66], V. Dobishuk[50], A.D. Docheva[57], A. Dolmatov[41], C. Dong[4], A.M. Donohoe[20], F. Dordei[29], A.C. dos Reis[2], L. Douglas[57], A.G. Downes[10], W. Duan[69], P. Duda[77], M.W. Dudek[38], L. Dufour[46], V. Duk[31], P. Durante[46], M.M. Duras[77], J.M. Durham[65], A. Dziurda[38], A. Dzyuba[41], S. Easo[55,46], E. Eckstein[73], U. Egede[1], A. Egorychev[41], V. Egorychev[41], C. Eirea Orro[44], S. Eisenhardt[56], E. Ejopu[60], S. Ek-In[47], L. Eklund[78], M. Elashri[63], J. Ellbracht[17], S. Ely[59], A. Ene[40], E. Epple[63], S. Escher[16], J. Eschle[48], S. Esen[19], T. Evans[60], F. Fabiano[29,j,46], L.N. Falcao[2], Y. Fan[7], B. Fang[71,13], L. Fantini[31,q], M. Faria[47], K. Farmer[56], D. Fazzini[28,o], L. Felkowski[77], M. Feng[5,7], M. Feo[46], M. Fernandez Gomez[44], A.D. Fernez[64], F. Ferrari[22], F. Ferreira Rodrigues[3], S. Ferreres Sole[35], M. Ferrillo[48], M. Ferro-Luzzi[46], S. Filippov[41], R.A. Fini[21], M. Fiorini[23,k], K.M. Fischer[61], D.S. Fitzgerald[79], C. Fitzpatrick[60], F. Fleuret[14], M. Fontana[22], L.F. Foreman[60], R. Forty[46], D. Foulds-Holt[53], M. Franco Sevilla[64], M. Frank[46], E. Franzoso[23,k], G. Frau[19], C. Frei[46], D.A. Friday[60], L. Frontini[27,n], J. Fu[7], Q. Fuehring[17], Y. Fujii[1], T. Fulghesu[15], E. Gabriel[35], G. Galati[21,h], M.D. Galati[35], A. Gallas Torreira[44], D. Galli[22,i], S. Gambetta[56], M. Gandelman[3], P. Gandini[27], H. Gao[7], R. Gao[61], Y. Gao[8], Y. Gao[6], Y. Gao[8], M. Garau[29,j], L.M. Garcia Martin[47], P. Garcia Moreno[43], J. García Pardiñas[46], B. Garcia Plana[44], K.G. Garg[8], L. Garrido[43], C. Gaspar[46], R.E. Geertsema[35], L.L. Gerken[17], E. Gersabeck[60], M. Gersabeck[60], T. Gershon[54], Z. Ghorbanimoghaddam[52], L. Giambastiani[30], F.I. Giasemis[15,e], V. Gibson[53], H.K. Giemza[39], A.L. Gilman[61], M. Giovannetti[25], A. Gioventù[43], P. Gironella Gironell[43], C. Giugliano[23,k], M.A. Giza[38], E.L. Gkougkousis[59], F.C. Glaser[13,19], V.V. Gligorov[15], C. Göbel[67], E. Golobardes[42], D. Golubkov[41], A. Golutvin[59,41,46], A. Gomes[2,a,†], S. Gomez Fernandez[43], F. Goncalves Abrantes[61], M. Goncerz[38], G. Gong[4], J.A. Gooding[17], I.V. Gorelov[41], C. Gotti[28], J.P. Grabowski[73], L.A. Granado Cardoso[46], E. Graugés[43], E. Graverini[47,s], L. Grazette[54], G. Graziani, A.T. Grecu[40], L.M. Greeven[35], N.A. Grieser[63], L. Grillo[57], S. Gromov[41], C. Gu[14], M. Guarise[23], M. Guittiere[13], V. Guliaeva[41], P.A. Günther[19], A.-K. Guseinov[41], E. Gushchin[41], Y. Guz[6,41,46], T. Gys[46], K. Habermann[73], T. Hadavizadeh[1], C. Hadjivasiliou[64], G. Haefeli[47], C. Haen[46], J. Haimberger[46], M. Hajheidari[46], M.M. Halvorsen[46], P.M. Hamilton[64], J. Hammerich[58], Q. Han[8], X. Han[19], S. Hansmann-Menzemer[19], L. Hao[7], N. Harnew[61], T. Harrison[58], M. Hartmann[13], J. He[7,c], K. Heijhoff[35], F. Hemmer[46], C. Henderson[63], R.D.L. Henderson[1,54], A.M. Hennequin[46], K. Hennessy[58], L. Henry[47], J. Herd[59], P. Herrero Gascon[19], J. Heuel[16], A. Hicheur[3], G. Hijano Mendizabal[48], D. Hill[47], S.E. Hollitt[17], J. Horswill[60], R. Hou[8], Y. Hou[10], N. Howarth[58], J. Hu[19], J. Hu[69], W. Hu[6], X. Hu[4], W. Huang[7], W. Hulsbergen[35], R.J. Hunter[54], M. Hushchyn[41], D. Hutchcroft[58], D. Ilin[41], P. Ilten[63], A. Inglessi[41], A. Iniukhin[41], A. Ishteev[41], K. Ivshin[41], R. Jacobsson[46], H. Jage[16], S.J. Jaimes Elles[45,72], S. Jakobsen[46], E. Jans[35], B.K. Jashal[45], A. Jawahery[64,46], V. Jevtic[17], E. Jiang[64], X. Jiang[5,7], Y. Jiang[7], Y.J. Jiang[6], M. John[61], D. Johnson[51], C.R. Jones[53], T.P. Jones[54], S. Joshi[39], B. Jost[46], N. Jurik[46], I. Juszczak[38], D. Kaminaris[47], S. Kandybei[49], Y. Kang[4], M. Karacson[46], D. Karpenkov[41], M. Karpov[41], A.M. Kauniskangas[47], J.W. Kautz[63], F. Keizer[46], D.M. Keller[66], M. Kenzie[53], T. Ketel[35], B. Khanji[66], A. Kharisova[41], S. Kholodenko[32], G. Khreich[13], T. Kirn[16], V.S. Kirsebom[47], O. Kitouni[62], S. Klaver[36], N. Kleijne[32,r], K. Klimaszewski[39], M.R. Kmiec[39], S. Koliiev[50],

2024 JINST 19 P02008

L. Kolk[17], A. Konoplyannikov[41], P. Kopciewicz[37,46], P. Koppenburg[35], M. Korolev[41], I. Kostiuk[35], O. Kot[50], S. Kotriakhova, A. Kozachuk[41], P. Kravchenko[41], L. Kravchuk[41], M. Kreps[54], S. Kretzschmar[16], P. Krokovny[41], W. Krupa[66], W. Krzemien[39], J. Kubat[19], S. Kubis[77], W. Kucewicz[38], M. Kucharczyk[38], V. Kudryavtsev[41], E. Kulikova[41], A. Kupsc[78], B.K. Kutsenko[12], D. Lacarrere[46], A. Lai[29], A. Lampis[29], D. Lancierini[48], C. Landesa Gomez[44], J.J. Lane[1], R. Lane[52], C. Langenbruch[19], J. Langer[17], O. Lantwin[41], T. Latham[54], F. Lazzari[32,s], C. Lazzeroni[51], R. Le Gac[12], S.H. Lee[79], R. Lefèvre[11], A. Leflat[41], S. Legotin[41], M. Lehuraux[54], O. Leroy[12], T. Lesiak[38], B. Leverington[19], A. Li[4], H. Li[69], K. Li[8], L. Li[60], P. Li[46], P.-R. Li[70], S. Li[8], T. Li[5,d], T. Li[69], Y. Li[8], Y. Li[5], Z. Li[66], Z. Lian[4], X. Liang[66], C. Lin[7], T. Lin[55], R. Lindner[46], V. Lisovskyi[47], R. Litvinov[29,j], F.L. Liu[1], G. Liu[69], K. Liu[70], Q. Liu[7], S. Liu[5,7], Y. Liu[56], Y. Liu[70], Y.L. Liu[59], A. Lobo Salvia[43], A. Loi[29], J. Lomba Castro[44], T. Long[53], J.H. Lopes[3], A. Lopez Huertas[43], S. López Soliño[44], G.H. Lovell[53], C. Lucarelli[24,l], D. Lucchesi[30,p], S. Luchuk[41], M. Lucio Martinez[76], V. Lukashenko[35,50], Y. Luo[6], A. Lupato[30], E. Luppi[23,k], K. Lynch[20], X.-R. Lyu[7], G.M. Ma[4], R. Ma[7], S. Maccolini[17], F. Machefert[13], F. Maciuc[40], B.M. Mack[66], I. Mackay[61], L.M. Mackey[66], L.R. Madhan Mohan[53], M.M. Madurai[51], A. Maevskiy[41], D. Magdalinski[35], D. Maisuzenko[41], M.W. Majewski[37], J.J. Malczewski[38], S. Malde[61], B. Malecki[38,46], L. Malentacca[46], A. Malinin[41], T. Maltsev[41], G. Manca[29,j], G. Mancinelli[12], C. Mancuso[27,13,n], R. Manera Escalero[43], D. Manuzzi[22], D. Marangotto[27,n], J.F. Marchand[10], R. Marchevski[47], U. Marconi[22], S. Mariani[46], C. Marin Benito[43], J. Marks[19], A.M. Marshall[52], P.J. Marshall[58], G. Martelli[31,q], G. Martellotti[33], L. Martinazzoli[46], M. Martinelli[28,o], D. Martinez Santos[44], F. Martinez Vidal[45], A. Massafferri[2], M. Materok[16], R. Matev[46], A. Mathad[48], V. Matiunin[41], C. Matteuzzi[66], K.R. Mattioli[14], A. Mauri[59], E. Maurice[14], J. Mauricio[43], P. Mayencourt[47], M. Mazurek[46], M. McCann[59], L. Mcconnell[20], T.H. McGrath[60], N.T. McHugh[57], A. McNab[60], R. McNulty[20], B. Meadows[63], G. Meier[17], D. Melnychuk[39], M. Merk[35,76], A. Merli[27,n], L. Meyer Garcia[3], D. Miao[5,7], H. Miao[7], M. Mikhasenko[73,f], D.A. Milanes[72], A. Minotti[28,o], E. Minucci[66], T. Miralles[11], S.E. Mitchell[56], B. Mitreska[17], D.S. Mitzel[17], A. Modak[55], A. Mödden[17], R.A. Mohammed[61], R.D. Moise[16], S. Mokhnenko[41], T. Mombächer[46], M. Monk[54,1], I.A. Monroy[72], S. Monteil[11], A. Morcillo Gomez[44], G. Morello[25], M.J. Morello[32,r], M.P. Morgenthaler[19], A.B. Morris[46], A.G. Morris[12], R. Mountain[66], H. Mu[4], Z.M. Mu[6], E. Muhammad[54], F. Muheim[56], M. Mulder[75], K. Müller[48], F. Mũnoz-Rojas[9], R. Murta[59], P. Naik[58], T. Nakada[47], R. Nandakumar[55], T. Nanut[46], I. Nasteva[3], M. Needham[56,*], N. Neri[27,n], S. Neubert[73], N. Neufeld[46], P. Neustroev[41], R. Newcombe[59], J. Nicolini[17,13], D. Nicotra[76], E.M. Niel[47], N. Nikitin[41], P. Nogga[73], N.S. Nolte[62], C. Normand[10,29], J. Novoa Fernandez[44], G. Nowak[63], C. Nunez[79], H.N. Nur[57], A. Oblakowska-Mucha[37], V. Obraztsov[41], T. Oeser[16], S. Okamura[23,k,46], R. Oldeman[29,j], F. Oliva[56], M. Olocco[17], C.J.G. Onderwater[76], R.H. O'Neil[56], J.M. Otalora Goicochea[3], T. Ovsiannikova[41], P. Owen[48], A. Oyanguren[45], O. Ozcelik[56], K.O. Padeken[73], B. Pagare[54], P.R. Pais[19], T. Pajero[61], A. Palano[21], M. Palutan[25], G. Panshin[41], L. Paolucci[54], A. Papanestis[55], M. Pappagallo[21,h], L.L. Pappalardo[23,k], C. Pappenheimer[63], C. Parkes[60], B. Passalacqua[23,k], G. Passaleva[24], D. Passaro[32,r], A. Pastore[21], M. Patel[59], J. Patoc[61], C. Patrignani[22,i], C.J. Pawley[76], A. Pellegrino[35], M. Pepe Altarelli[25], S. Perazzini[22], D. Pereima[41], A. Pereiro Castro[44], P. Perret[11], A. Perro[46], K. Petridis[52], A. Petrolini[26,m], S. Petrucci[56], J.P. Pfaller[63], H. Pham[66], L. Pica[32,r], M. Piccini[31],

2024 JINST 19 P02008

B. Pietrzyk[10], G. Pietrzyk[13], D. Pinci[33], F. Pisani[46], M. Pizzichemi[28,o], V. Placinta[40], M. Plo Casasus[44], F. Polci[15,46], M. Poli Lener[25], A. Poluektov[12], N. Polukhina[41], I. Polyakov[46], E. Polycarpo[3], S. Ponce[46], D. Popov[7], S. Poslavskii[41], K. Prasanth[38], C. Prouve[44], V. Pugatch[50], G. Punzi[32,s], W. Qian[7], N. Qin[4], S. Qu[4], R. Quagliani[47], R.I. Rabadan Trejo[54], J.H. Rademacker[52], M. Rama[32], M. Ramírez García[79], M. Ramos Pernas[54], M.S. Rangel[3], F. Ratnikov[41], G. Raven[36], M. Rebollo De Miguel[45], F. Redi[46], J. Reich[52], F. Reiss[60], Z. Ren[7], P.K. Resmi[61], R. Ribatti[32,r], G.R. Ricart[14,80], D. Riccardi[32,r], S. Ricciardi[55], K. Richardson[62], M. Richardson-Slipper[56], K. Rinnert[58], P. Robbe[13], G. Robertson[57], E. Rodrigues[58,46], E. Rodriguez Fernandez[44], J.A. Rodriguez Lopez[72], E. Rodriguez Rodriguez[44], A. Rogovskiy[55], D.L. Rolf[46], A. Rollings[61], P. Roloff[46], V. Romanovskiy[41], M. Romero Lamas[44], A. Romero Vidal[44], G. Romolini[23], F. Ronchetti[47], M. Rotondo[25], S.R. Roy[19], M.S. Rudolph[66], T. Ruf[46], M. Ruiz Diaz[19], R.A. Ruiz Fernandez[44], J. Ruiz Vidal[78,z], A. Ryzhikov[41], J. Ryzka[37], J.J. Saborido Silva[44], R. Sadek[14], N. Sagidova[41], N. Sahoo[51], B. Saitta[29,j], M. Salomoni[28,o], C. Sanchez Gras[35], I. Sanderswood[45], R. Santacesaria[33], C. Santamarina Rios[44], M. Santimaria[25], L. Santoro[2], E. Santovetti[34], A. Saputi[23,46], D. Saranin[41], G. Sarpis[56], M. Sarpis[73], A. Sarti[33], C. Satriano[33,t], A. Satta[34], M. Saur[6], D. Savrina[41], H. Sazak[11], L.G. Scantlebury Smead[61], A. Scarabotto[15], S. Schael[16], S. Scherl[58], A.M. Schertz[74], M. Schiller[57], H. Schindler[46], M. Schmelling[18], B. Schmidt[46], S. Schmitt[16], H. Schmitz[73], O. Schneider[47], A. Schopper[46], N. Schulte[17], S. Schulte[47], M.H. Schune[13], R. Schwemmer[46], G. Schwering[16], B. Sciascia[25], A. Sciuccati[46], S. Sellam[44], A. Semennikov[41], M. Senghi Soares[36], A. Sergi[26,m], N. Serra[48,46], L. Sestini[30], A. Seuthe[17], Y. Shang[6], D.M. Shangase[79], M. Shapkin[41], R.S. Sharma[66], I. Shchemerov[41], L. Shchutska[47], T. Shears[58], L. Shekhtman[41], Z. Shen[6], S. Sheng[5,7], V. Shevchenko[41], B. Shi[7], E.B. Shields[28,o], Y. Shimizu[13], E. Shmanin[41], R. Shorkin[41], J.D. Shupperd[66], R. Silva Coutinho[66], G. Simi[30], S. Simone[21,h], N. Skidmore[60], R. Skuza[19], T. Skwarnicki[66], M.W. Slater[51], J.C. Smallwood[61], E. Smith[62], K. Smith[65], M. Smith[59], A. Snoch[35], L. Soares Lavra[56], M.D. Sokoloff[63], F.J.P. Soler[57], A. Solomin[41,52], A. Solovev[41], I. Solovyev[41], R. Song[1], Y. Song[47], Y. Song[4], Y.S. Song[6], F.L. Souza De Almeida[66], B. Souza De Paula[3], E. Spadaro Norella[27,n], E. Spedicato[22], J.G. Speer[17], E. Spiridenkov[41], P. Spradlin[57], V. Sriskaran[46], F. Stagni[46], M. Stahl[46], S. Stahl[46], S. Stanislaus[61], E.N. Stein[46], O. Steinkamp[48], O. Stenyakin[41], H. Stevens[17], D. Strekalina[41], Y. Su[7], F. Suljik[61], J. Sun[29], L. Sun[71], Y. Sun[64], P.N. Swallow[51], F. Swystun[54], A. Szabelski[39], T. Szumlak[37], M. Szymanski[46], Y. Tan[4], S. Taneja[60], M.D. Tat[61], A. Terentev[48], F. Terzuoli[32,v], F. Teubert[46], E. Thomas[46], D.J.D. Thompson[51], H. Tilquin[59], V. Tisserand[11], S. T'Jampens[10], M. Tobin[5], L. Tomassetti[23,k], G. Tonani[27,n,46], X. Tong[6], D. Torres Machado[2], L. Toscano[17], D.Y. Tou[4], C. Trippl[42], G. Tuci[19], N. Tuning[35], L.H. Uecker[19], A. Ukleja[37], D.J. Unverzagt[19], E. Ursov[41], A. Usachov[36], A. Ustyuzhanin[41], U. Uwer[19], V. Vagnoni[22], A. Valassi[46], G. Valenti[22], N. Valls Canudas[42], H. Van Hecke[65], E. van Herwijnen[59], C.B. Van Hulse[44,x], R. Van Laak[47], M. van Veghel[35], R. Vazquez Gomez[43], P. Vazquez Regueiro[44], C. Vázquez Sierra[44], S. Vecchi[23], J.J. Velthuis[52], M. Veltri[24,w], A. Venkateswaran[47], M. Vesterinen[54], M. Vieites Diaz[46], X. Vilasis-Cardona[42], E. Vilella Figueras[58], A. Villa[22], P. Vincent[15], F.C. Volle[13], D. vom Bruch[12], V. Vorobyev[41], N. Voropaev[41], K. Vos[76], G. Vouters[10], C. Vrahas[56], J. Walsh[32], E.J. Walton[1], G. Wan[6], C. Wang[19], G. Wang[8], J. Wang[6], J. Wang[5], J. Wang[4], J. Wang[71], M. Wang[27], N.W. Wang[7], R. Wang[52], X. Wang[69], X.W. Wang[59], Y. Wang[8], Z. Wang[13],

Z. Wang[4], Z. Wang[7], J.A. Ward[54,1], M. Waterlaat[46], N.K. Watson[51], D. Websdale[59], Y. Wei[6], B.D.C. Westhenry[52], D.J. White[60], M. Whitehead[57], A.R. Wiederhold[54], D. Wiedner[17], G. Wilkinson[61], M.K. Wilkinson[63], M. Williams[62], M.R.J. Williams[56], R. Williams[53], F.F. Wilson[55], W. Wislicki[39], M. Witek[38], L. Witola[19], C.P. Wong[65], G. Wormser[13], S.A. Wotton[53], H. Wu[66], J. Wu[8], Y. Wu[6], K. Wyllie[46], S. Xian[69], Z. Xiang[5], Y. Xie[8], A. Xu[32], J. Xu[7], L. Xu[4], L. Xu[4], M. Xu[54], Z. Xu[11], Z. Xu[7], Z. Xu[5], D. Yang[4], S. Yang[7], X. Yang[6], Y. Yang[26,m], Z. Yang[6], Z. Yang[64], V. Yeroshenko[13], H. Yeung[60], H. Yin[8], C.Y. Yu[6], J. Yu[68], X. Yuan[5], E. Zaffaroni[47], M. Zavertyaev[18], M. Zdybal[38], M. Zeng[4], C. Zhang[6], D. Zhang[8], J. Zhang[7], L. Zhang[4], S. Zhang[68], S. Zhang[6], Y. Zhang[6], Y.Z. Zhang[4], Y. Zhao[19], A. Zharkova[41], A. Zhelezov[19], X.Z. Zheng[4], Y. Zheng[7], T. Zhou[6], X. Zhou[8], Y. Zhou[7], V. Zhovkovska[54], L.Z. Zhu[7], X. Zhu[4], X. Zhu[8], V. Zhukov[16,41], J. Zhuo[45], Q. Zou[5,7], D. Zuliani[30], G. Zunica[60]

[1] *School of Physics and Astronomy, Monash University, Melbourne, Australia*
[2] *Centro Brasileiro de Pesquisas Físicas (CBPF), Rio de Janeiro, Brazil*
[3] *Universidade Federal do Rio de Janeiro (UFRJ), Rio de Janeiro, Brazil*
[4] *Center for High Energy Physics, Tsinghua University, Beijing, China*
[5] *Institute Of High Energy Physics (IHEP), Beijing, China*
[6] *School of Physics State Key Laboratory of Nuclear Physics and Technology, Peking University, Beijing, China*
[7] *University of Chinese Academy of Sciences, Beijing, China*
[8] *Institute of Particle Physics, Central China Normal University, Wuhan, Hubei, China*
[9] *Consejo Nacional de Rectores (CONARE), San Jose, Costa Rica*
[10] *Université Savoie Mont Blanc, CNRS, IN2P3-LAPP, Annecy, France*
[11] *Université Clermont Auvergne, CNRS/IN2P3, LPC, Clermont-Ferrand, France*
[12] *Aix Marseille Univ, CNRS/IN2P3, CPPM, Marseille, France*
[13] *Université Paris-Saclay, CNRS/IN2P3, IJCLab, Orsay, France*
[14] *Laboratoire Leprince-Ringuet, CNRS/IN2P3, Ecole Polytechnique, Institut Polytechnique de Paris, Palaiseau, France*
[15] *LPNHE, Sorbonne Université, Paris Diderot Sorbonne Paris Cité, CNRS/IN2P3, Paris, France*
[16] *I. Physikalisches Institut, RWTH Aachen University, Aachen, Germany*
[17] *Fakultät Physik, Technische Universität Dortmund, Dortmund, Germany*
[18] *Max-Planck-Institut für Kernphysik (MPIK), Heidelberg, Germany*
[19] *Physikalisches Institut, Ruprecht-Karls-Universität Heidelberg, Heidelberg, Germany*
[20] *School of Physics, University College Dublin, Dublin, Ireland*
[21] *INFN Sezione di Bari, Bari, Italy*
[22] *INFN Sezione di Bologna, Bologna, Italy*
[23] *INFN Sezione di Ferrara, Ferrara, Italy*
[24] *INFN Sezione di Firenze, Firenze, Italy*
[25] *INFN Laboratori Nazionali di Frascati, Frascati, Italy*
[26] *INFN Sezione di Genova, Genova, Italy*
[27] *INFN Sezione di Milano, Milano, Italy*
[28] *INFN Sezione di Milano-Bicocca, Milano, Italy*
[29] *INFN Sezione di Cagliari, Monserrato, Italy*
[30] *Università degli Studi di Padova, Università e INFN, Padova, Padova, Italy*
[31] *INFN Sezione di Perugia, Perugia, Italy*
[32] *INFN Sezione di Pisa, Pisa, Italy*
[33] *INFN Sezione di Roma La Sapienza, Roma, Italy*
[34] *INFN Sezione di Roma Tor Vergata, Roma, Italy*
[35] *Nikhef National Institute for Subatomic Physics, Amsterdam, Netherlands*
[36] *Nikhef National Institute for Subatomic Physics and VU University Amsterdam, Amsterdam, Netherlands*
[37] *AGH — University of Science and Technology, Faculty of Physics and Applied Computer Science, Kraków, Poland*
[38] *Henryk Niewodniczanski Institute of Nuclear Physics Polish Academy of Sciences, Kraków, Poland*

2024 JINST 19 P02008

[39] National Center for Nuclear Research (NCBJ), Warsaw, Poland
[40] Horia Hulubei National Institute of Physics and Nuclear Engineering, Bucharest-Magurele, Romania
[41] Affiliated with an institute covered by a cooperation agreement with CERN
[42] DS4DS, La Salle, Universitat Ramon Llull, Barcelona, Spain
[43] ICCUB, Universitat de Barcelona, Barcelona, Spain
[44] Instituto Galego de Física de Altas Enerxías (IGFAE), Universidade de Santiago de Compostela, Santiago de Compostela, Spain
[45] Instituto de Fisica Corpuscular, Centro Mixto Universidad de Valencia - CSIC, Valencia, Spain
[46] European Organization for Nuclear Research (CERN), Geneva, Switzerland
[47] Institute of Physics, Ecole Polytechnique Fédérale de Lausanne (EPFL), Lausanne, Switzerland
[48] Physik-Institut, Universität Zürich, Zürich, Switzerland
[49] NSC Kharkiv Institute of Physics and Technology (NSC KIPT), Kharkiv, Ukraine
[50] Institute for Nuclear Research of the National Academy of Sciences (KINR), Kyiv, Ukraine
[51] University of Birmingham, Birmingham, United Kingdom
[52] H.H. Wills Physics Laboratory, University of Bristol, Bristol, United Kingdom
[53] Cavendish Laboratory, University of Cambridge, Cambridge, United Kingdom
[54] Department of Physics, University of Warwick, Coventry, United Kingdom
[55] STFC Rutherford Appleton Laboratory, Didcot, United Kingdom
[56] School of Physics and Astronomy, University of Edinburgh, Edinburgh, United Kingdom
[57] School of Physics and Astronomy, University of Glasgow, Glasgow, United Kingdom
[58] Oliver Lodge Laboratory, University of Liverpool, Liverpool, United Kingdom
[59] Imperial College London, London, United Kingdom
[60] Department of Physics and Astronomy, University of Manchester, Manchester, United Kingdom
[61] Department of Physics, University of Oxford, Oxford, United Kingdom
[62] Massachusetts Institute of Technology, Cambridge, MA, United States
[63] University of Cincinnati, Cincinnati, OH, United States
[64] University of Maryland, College Park, MD, United States
[65] Los Alamos National Laboratory (LANL), Los Alamos, NM, United States
[66] Syracuse University, Syracuse, NY, United States
[67] Pontifícia Universidade Católica do Rio de Janeiro (PUC-Rio), Rio de Janeiro, Brazil, associated to [3]
[68] School of Physics and Electronics, Hunan University, Changsha City, China, associated to [8]
[69] Guangdong Provincial Key Laboratory of Nuclear Science, Guangdong-Hong Kong Joint Laboratory of Quantum Matter, Institute of Quantum Matter, South China Normal University, Guangzhou, China, associated to [4]
[70] Lanzhou University, Lanzhou, China, associated to [5]
[71] School of Physics and Technology, Wuhan University, Wuhan, China, associated to [4]
[72] Departamento de Fisica , Universidad Nacional de Colombia, Bogota, Colombia, associated to [15]
[73] Universität Bonn - Helmholtz-Institut für Strahlen und Kernphysik, Bonn, Germany, associated to [19]
[74] Eotvos Lorand University, Budapest, Hungary, associated to [46]
[75] Van Swinderen Institute, University of Groningen, Groningen, Netherlands, associated to [35]
[76] Universiteit Maastricht, Maastricht, Netherlands, associated to [35]
[77] Tadeusz Kosciuszko Cracow University of Technology, Cracow, Poland, associated to [38]
[78] Department of Physics and Astronomy, Uppsala University, Uppsala, Sweden, associated to [57]
[79] University of Michigan, Ann Arbor, MI, United States, associated to [66]
[80] Departement de Physique Nucleaire (SPhN), Gif-Sur-Yvette, France

[a] Universidade de Brasília, Brasília, Brazil
[b] Centro Federal de Educacão Tecnológica Celso Suckow da Fonseca, Rio De Janeiro, Brazil
[c] Hangzhou Institute for Advanced Study, UCAS, Hangzhou, China
[d] School of Physics and Electronics, Henan University , Kaifeng, China
[e] LIP6, Sorbonne Universite, Paris, France
[f] Excellence Cluster ORIGINS, Munich, Germany
[g] Universidad Nacional Autónoma de Honduras, Tegucigalpa, Honduras
[h] Università di Bari, Bari, Italy
[i] Università di Bologna, Bologna, Italy

[j] Università di Cagliari, Cagliari, Italy
[k] Università di Ferrara, Ferrara, Italy
[l] Università di Firenze, Firenze, Italy
[m] Università di Genova, Genova, Italy
[n] Università degli Studi di Milano, Milano, Italy
[o] Università di Milano Bicocca, Milano, Italy
[p] Università di Padova, Padova, Italy
[q] Università di Perugia, Perugia, Italy
[r] Scuola Normale Superiore, Pisa, Italy
[s] Università di Pisa, Pisa, Italy
[t] Università della Basilicata, Potenza, Italy
[u] Università di Roma Tor Vergata, Roma, Italy
[v] Università di Siena, Siena, Italy
[w] Università di Urbino, Urbino, Italy
[x] Universidad de Alcalá, Alcalá de Henares , Spain
[y] Universidade da Coruña, Coruña, Spain
[z] Department of Physics/Division of Particle Physics, Lund, Sweden
[†] Deceased
[*] Corresponding author

2024 JINST 19 P02008